ChemComm

Cite this: *Chem. Commun.*, 2011, **47**, 11918–11920

www.rsc.org/chemcomm

COMMUNICATION

Application of synchrotron FTIR microspectroscopy for determination of spatial distribution of methylene blue conjugated onto a SAM *via* "click" chemistry†

Socrates Jose P. Cañete,[a] Zhengzheng Zhang,[b] Lingmei Kong,[b] Vicki L. Schlegel,[c] Bradley A. Plantz,[d] Peter A. Dowben[b] and Rebecca Y. Lai*[a]

Received 1st June 2011, Accepted 20th September 2011
DOI: 10.1039/c1cc13255e

We report, for the first time, the application of synchrotron FTIR microspectroscopy to determine the spatial distribution of methylene blue conjugated onto a self-assembled monolayer surface *via* Sharpless "click" chemistry.

Sharpless "click" chemistry has been one of the most versatile and indispensable chemistry tools in organic synthesis since its discovery in 2001.[1] More recently, the use of "click" chemistry in surface modification has been proposed and realized.[2,3] One such application is the fabrication of biosensors. In this sensor fabrication approach, a self-assembled monolayer (SAM) containing surface-active azide moieties is first formed on a gold surface, followed by conjugation of the biosensing elements onto the azide-containing SAM.[4] This approach has been demonstrated to be well-suited for the fabrication of an electrochemical DNA (E-DNA) sensor. The "click"-based E-DNA sensor exhibits similar sensor properties when compared to the E-DNA sensor fabricated *via* the conventional "two step" approach, which involves direct adsorption of thiolated DNA probes onto the gold electrode.[5] Similar to most surface-based biosensors, the "click"-based E-DNA sensor performance is highly dependent on the total probe coverage and more importantly, the distribution of the probes on the sensor surface.[6–8] We thus believe sensor performance can be greatly enhanced by simply adjusting the probe coverage and spatial distribution—which are governed by the surface concentration and distribution of the active azide moieties on the SAM surface.

[a] *Department of Chemistry, University of Nebraska-Lincoln, Lincoln, NE, USA. E-mail: rlai2@unl.edu; Fax: +1-402-472-9402; Tel: +1-402-472-5340*
[b] *Department of Physics and Astronomy, University of Nebraska-Lincoln, Lincoln, NE, USA. E-mail: dowben@unl.edu; Fax: +1-402-472-6148; Tel: +1-402-472-9838*
[c] *Food Science and Technology Department, University of Nebraska-Lincoln, Lincoln, NE, USA. E-mail: vlschleg@unlnotes.unl.edu; Fax: +1-402-472-1693; Tel: +1-402-416-0294*
[d] *School of Biological Sciences, University of Nebraska-Lincoln, Lincoln, NE, USA. E-mail: bplantz2@unl.edu; Fax: +1-402-472-2083; Tel: +1-402-472-2253*

† Electronic supplementary information (ESI) available: Description of experimental methods and structure of C7-MB. See DOI: 10.1039/c1cc13255e

To date, various surface analysis techniques, including atomic force microscopy and scanning tunnelling microscopy, have been utilized in the characterization of probe distribution on SAMs.[9,10] Fourier transform infrared microspectroscopy (FTIR-M), a technique that combines light microscopy and infrared spectroscopy, will undoubtedly be a valuable tool in determining biosensing probe coverage and distribution.[11] However, in an FTIR-M experiment, the aperture size is greatly reduced, thereby limiting the IR flux that reaches the detector, leading to a decrease in the S/N ratio. Thus, to enhance the sensitivity of the signal and resolution of the recorded image, a synchrotron radiation source is often employed, owing to its effective brightness that is 100–1000 times higher than conventional thermal sources.[12,13] Here we report, for the first time, the application of synchrotron FTIR and FTIR-M to determine the spatial distribution of an alkyne-modified MB (C7-MB) conjugated to a SAM-modified electrode *via* "click" chemistry (Fig. S1, ESI†).

In this study, mixed SAMs consisted of 11-hydroxy-undecane-thiol (C11-OH) and 11-azido-undecane-thiol (C11-N_3) were formed on gold-coated silicon wafers (gold substrates). The SAMs were deposited in a stepwise fashion; the piranha-cleaned gold substrates were first incubated in C11-N_3 (*P*-0) or a mixture of C11-OH and C11-N_3 (*P*-3h) for 10 min. The partially-coated gold substrates were then incubated in C11-OH for 3 h to complete the SAM formation (Fig. S2, ESI†). The SAMs resulting from the two protocols are expected to be different. The absence of C11-OH in the first incubation step promotes formation of C11-N_3 clusters on the gold surface; the P-0 SAM is thus presumed to be a less homogeneous monolayer when compared to the P-3h SAM. In addition, owing to the lack of competition in the adsorption between the two thiols, the P-0 SAM should also display a higher concentration of surface azides. Here we employed X-ray photoelectron spectroscopy (XPS) to determine the relative concentration of surface azide between the two SAMs.[4] Of note, data collection times and the X-ray flux were specifically limited to avoid X-ray induced molecular fragmentation, which in turn diminished the signal-to-noise but preserved sample quality. Nevertheless, the presence of the two signature N (1s) peaks at 405 and 402 eV validates the presence of azide,

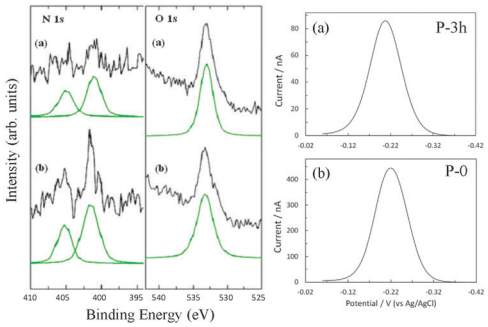

Fig. 1 (Left) Experimental XPS spectra (black) and corresponding best-fit curves (green) of element N 1s and O 1s for (a) P-3h and (b) P-0 SAMs. (Right) AC voltammograms of C7-MB conjugated onto (a) P-3h and (b) P-0 SAMs (AC frequency: 10 Hz, amplitude: 25 mV).

with a screened and unscreened final state consistent with placement as a terminal group on the alkane end away from the metal substrate. The O (1s) core level peak at 532 eV signifies the presence of a bonded oxygen species. The presence of these chemically specific spectra signatures clearly indicates that both monolayers contain C11-N_3 and C11-OH (Fig. 1a). Relative abundance of the two thiols, however, differs significantly between the two SAMs. The calculated abundance of azide relative to oxygen is 0.7665 for the P-3h SAM and 1.6382 for the P-0 SAM, indicating that the P-3h SAM contains fewer surface azides when compared to the P-0 SAM.

To correlate the abundance of surface azide to C7-MB probe density, we deposited both P-0 and P-3h SAMs on gold disk electrodes well-suited for electrochemical characterization.[5] The resultant monolayers were then subjected to the "click" reaction for direct conjugation of the C7-MB probes (Fig. S1, ESI†). The electrochemical signal of the C7-MB probes was monitored using alternating current voltammetry (ACV). As shown in Fig. 1b, the MB reduction current observed with the P-0 SAM is higher than that obtained with the P-3h SAM. The average probe coverages for the P-0 and P-3h SAMs are 2.9×10^{12} and 4.2×10^{11} molecules/cm^2, respectively. These data are in accordance with the XPS results, suggesting that the amount of C7-MB conjugated onto the monolayer is highly dependent on the amount of available surface azide, which is contingent on the monolayer preparation strategy. However, while the overall probe coverage can affect sensor behaviour; it is often the distribution of the probes on the surface that is detrimental to sensor performance.

Thus, to determine the surface distribution of C7-MB, the two SAMs were deposited on a separate set of gold substrates, C7-MB was subsequently conjugated to the monolayers *via* "click" chemistry. These two monolayers were then analysed using synchrotron radiation-based FTIR and FTIR-M. Prior to the FTIR-M experiments, a conventional IR spectrum of the "free" C7-MB (*i.e.*, not conjugated to a surface) was collected and systematically characterized. The purpose of this experiment is twofold; first, it is necessary to generate a reference spectrum for MB, since the same spectral signatures will be monitored in the synchrotron FTIR-M experiment. Second, the resultant spectrum can be used to confirm the success of the actual "click" reaction, which is signified by the presence of spectral signatures of the 1,2,3-triazole ring.

Fig. 2 shows the normalized IR spectra of the "free" C7-MB and C7-MB conjugated onto a P-3h SAM-modified gold substrate. Despite the differences in the samples being analysed and the instruments used to collect the spectra, both spectra display broad bands in the 3200–3600 cm^{-1} region, presumably contributed by the overlapping stretches of N–H, O–H, and ═C–H aromatic groups found in C7-MB (Fig. S1, ESI†). Although characteristic alkyl C–H peaks (2800–3000 cm^{-1}) are present in both spectra, the relatively higher peak intensity and the slight shift (2895 cm^{-1}) observed with the conjugated C7-MB (Fig. 2b) could be due to the linker. The peaks observed in the fingerprint region of 600–1800 cm^{-1} appear to be more complex in the conjugated C7-MB spectrum, which could be attributed to the conjugation of the molecule to the monolayer. A notable difference between the two spectra is the presence of the triplet peaks in the "free" C7-MB spectrum, indicating the presence of amide I/II stretching/bending C═O and N–H modes (1632, 1657 cm^{-1}) and the MB aromatic group (1603 cm^{-1}). These three peaks, however, merge into one relatively less intense peak at 1631 cm^{-1} in the conjugated C7-MB spectrum. A recent study reported by Choi *et al.* showed a similar change in the IR spectral signature upon linking an azido fluorobenzoic acid ester to a silicon nanoparticle.[14] Furthermore, there are several peaks in both spectra that are indicative of the C7-MB moiety, these include heterocyclic vibrations of the MB skeleton (1340–1440 cm^{-1}, 1040–1100 cm^{-1}), heterocyclic CH bending vibrations (830–840 cm^{-1}), C–N aromatic stretches (1250–1300 cm^{-1}), and C–N and/or P═O modes (1100 cm^{-1}).[15,16] Infrared bands of the triazole anion have been reported to be near or within these regions (840, 1068, 1097, 1230, 1412, 1439 cm^{-1}), which could account for the minor band shifts and greater relative intensities of several bands for the conjugated C7-MB relative to the "free" C7-MB.[17] Other spectral signatures that confirm the successful conjugation of C7-MB onto the azide-containing SAM includes the presence of the alkyne band at 690 cm^{-1} in the "free" C7-MB spectrum, which is clearly absent in the conjugated C7-MB spectrum. The absence of the azide band at 2100 cm^{-1} and the appearance of the triazole anion marker band at 1145 cm^{-1} in the conjugated C7-MB spectrum provide key evidence in support of the successful "click" reaction.[17,18]

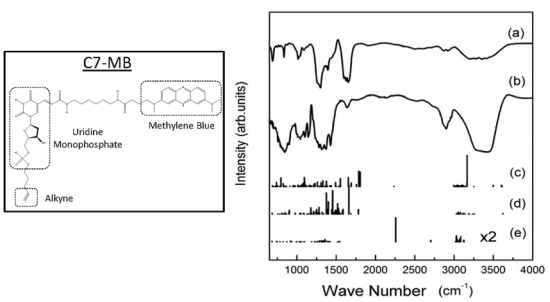

Fig. 2 (Left) Structure of C7-MB. (Right) Comparison of (a) the IR spectrum of "free" C7-MB and (b) synchrotron radiation-based FTIR spectrum of C7-MB conjugated onto a P-3h SAM-modified gold substrate. The calculated dipole active modes of the alkyne-modified MB (C7-MB) are shown divided to show those modes resulting from (c) the uridine monophosphate and alkyne moieties, (d) the MB moiety, and (e) the anchoring C11-N_3 moiety.

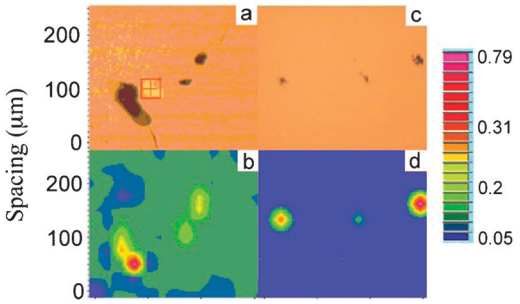

Fig. 3 Optical microscopy (a,c) and synchrotron radiation-based FTIR spatial spectra-microcroscopy (b,d) images of P-0 (a,b) and P-3h (c,d) SAMs modified with C7-MB *via* "click" chemistry. Absorbance of the characteristic MB 1428 cm^{-1} IR mode is indicated by colour (blue indicates low MB concentration and red indicates high MB concentration).

As a guide to the interpretation of the experimental data, we performed simple model calculations of both the vibrational modes and electronic structure of C7-MB and C11-N_3 (Fig. 2c, d and e, Fig. S3, ESI†). The oscillator strengths and eigen values of the dipole active modes for the C7-MB molecule and C11-N_3 were calculated using density functional theory (DFT) using a standard 6-31G* basis set. As observed, our experimental results are in reasonable agreement with both literature values and model calculations.

Fig. 3 shows the relative concentration and spatial distribution of C7-MB conjugated onto the P-0 and P-3h SAMs. The colour density of the features in the images is dependent on the concentration of surface immobilized C7-MB. As observed, there is far more clustering of the IR signature of C7-MB in the P-0 image and far more overall absorbance than that obtained with the P-3h SAM. Not only is more C7-MB conjugated onto the P-0 SAM surface, but as prepared, the azide-terminated thiol clusters. For the P-3h SAM, the absorbance (colour) is less intense and the spots are more uniformly distributed, suggesting that fewer C7-MB molecules are on the surface. These results are not unexpected since it is highly probable that there are surface aggregates of C11-N_3 in both SAMs, specifically, the P-0 SAM. It should be noted that the monolayer immobilization protocol employed here is a two-step process; in forming a P-0 SAM, the electrode is first exposed to only C11-N_3, the incorporation of C11-OH in the second step could further induce the semi-assembled C11-N_3 layer to cluster as the C11-OH molecules fill in the exposed gold surface, in addition to displacing some of the weakly bound C11-N_3 molecules. Consequently, higher surface concentration of C7-MB will be found in regions where aggregates of C11-N_3 are present.

However, for the P-3h SAM, incorporation of C11-OH in the first step has proven to be advantageous in forming a relatively well-mixed monolayer, with fewer aggregates of C11-N_3. Previous reports have established that in the formation of a mixed monolayer with two different thiols simultaneously present in the immobilization solution, competitive adsorption between the two thiols is inevitable.[19,20] In this case, C11-OH acted as the true "diluent" by lowering the total number of adsorbed C11-N_3, in addition to allowing them to be more evenly-spaced on the electrode surface. Nonetheless, the introduction of C11-OH in the second step could still cause C11-N_3 to aggregate, although to a lesser extent when compared to the P-0 SAM. Thus, the observed signal from C7-MB is less intense for this SAM system, as reflected by the lighter and more dispersed spots in the FTIR-M image.

In conclusion, despite the versatility and simplicity afforded by the "click" chemistry approach in sensor fabrication, careful consideration must be given to the design and fabrication of the monolayer if uniform distribution of biosensing elements on the sensor surface is desired. For this specific system, the incorporation of "diluents" in the SAM formation step has proven to be advantageous in producing a more homogeneous mixed monolayer, which is often required for the fabrication of folding-based electrochemical biosensors.[5–8] More importantly, this study highlights the use of FTIR-M in biosensing and surface science research. This technique is highly versatile and can be implemented in the analysis of monolayer surfaces other than the thiolated SAMs used in this study. It can also be employed to evaluate the efficiency of new surface conjugation approaches for applications that encompass both biosensing and material science research.

The authors acknowledge the support of National Science Foundation (NSF) (CHE-0909580), NSF MRSEC (DMR-0820521), and Nebraska EPSCoR (EPS-1004094).

Notes and references

1 H. C. Kolb, M. G. Finn and K. B. Sharpless, *Angew. Chem., Int. Ed.*, 2001, **40**, 2004–2021.
2 W. H. Binder and R. Sachsenhofer, *Macromol. Rapid Commun.*, 2007, **28**, 15–54.
3 H. Nandivada, X. Jiang and J. Lahann, *Adv. Mater.*, 2007, **19**, 2197–2208.
4 J. P. Collman, N. K. Devaraj, T. P. A. Eberspacher and C. E. D. Chidsey, *Langmuir*, 2006, **22**, 2457–2464.
5 S. S. J. P. Cañete, W. Yang and R. Y. Lai, *Chem. Commun.*, 2009, 4835–4837.
6 F. Ricci, R. Y. Lai, A. J. Heeger, K. W. Plaxco and J. J. Sumner, *Langmuir*, 2007, **23**, 6827–6834.
7 S. J. P. Cañete and R. Y. Lai, *Chem. Commun.*, 2010, **46**, 3941–3943.
8 W. Yang and R. Y. Lai, *Analyst*, 2011, **136**, 134–139.
9 Z.-L. Zhang, D.-W. Pang, R.-Y. Zhang, J.-W. Yan, B.-W. Mao and Y.-P. Qi, *Bioconjugate Chem.*, 2002, **13**, 104–109.
10 H. G. Hansma and J. H. Hoh, *Annu. Rev. Biophys. Biomol. Struct.*, 1994, **23**, 115–139.
11 J. E. Katon, *Micron*, 1996, **27**, 303–314.
12 P. Dumas, G. D. Sockalingum and J. Sule-Suso, *Trends Biotechnol.*, 2007, **25**, 40–44.
13 P. Dumas and L. Miller, *J. Biol. Phys.*, 2003, **29**, 201–208.
14 J. Choi, N. S. Wang and V. Reipa, *Bioconjugate Chem.*, 2008, **19**, 680–685.
15 O. V. Ovchinnidov, S. V. Chernykh, M. S. Smirnov, D. V. Alpatove, R. P. Vorob'eva, A. N. Latyshev, A. B. Evlev, A. N. Utekhin and A. N. Lukin, *J. Appl. Spectrosc.*, 2007, **74**, 809–815.
16 E. Saez and R. Corn, *Electrochim. Acta*, 1993, **38**, 1619–1625.
17 C. Tornkvist, J. Bergman and B. Liedberg, *J. Phys. Chem.*, 1991, **95**, 3119–3123.
18 D. A. Fleming, C. J. Thode and M. E. Williams, *Chem. Mater.*, 2006, **18**, 2327–2334.
19 J. P. Folkers, P. E. Laibinis, G. M. Whitesides and J. Deutch, *J. Phys. Chem.*, 1994, **98**, 563–571.
20 J. P. Folkers, P. E. Laibinis and George M. Whitesides, *Langmuir*, 1992, **8**, 1330–1341.